Liquid Crystals
Publication details, including instructions for authors and subscription information:
http://www.informaworld.com/smpp/title~content=t713926090

The rotational-conformational distribution of 2,2'-bithienyl in liquid crystals

Roberto Berardi[a]; Francesco Spinozzi[a]; Claudio Zannoni[a]
[a] Dipartimento di Chimica, Fisica ed Inorganica, Università, Bologna, Italy

To cite this Article Berardi, Roberto , Spinozzi, Francesco and Zannoni, Claudio(1994) 'The rotational-conformational distribution of 2,2'-bithienyl in liquid crystals', Liquid Crystals, 16: 3, 381 — 397
To link to this Article: DOI: 10.1080/02678299408029163
URL: http://dx.doi.org/10.1080/02678299408029163

LIQUID CRYSTALS, 1994, VOL. 16, NO. 3, 381–397

The rotational-conformational distribution of 2,2′-bithienyl in liquid crystals

by ROBERTO BERARDI, FRANCESCO SPINOZZI and CLAUDIO ZANNONI*

Dipartimento di Chimica Fisica ed Inorganica, Università, Viale Risorgimento, 4, 40136 Bologna, Italy

(*Received 5 August 1993; accepted 3 September 1993*)

We have investigated the distribution of conformations and orientations for a simple internal rotor molecule, 2,2′-bithienyl dissolved in liquid crystal solvents, by re-analysing published proton dipolar coupling data with the maximum entropy internal order method (MEIO). We show that detailed, model independent, conformational information can be obtained when data of sufficiently high quality are available. We also propose a novel and convenient representation method for the orientational-conformational coupling.

1. Introduction

The study of molecular structure and conformation in fluid phases is an important classical problem that has been attacked with a variety of techniques [1]. The use of NMR of molecules dissolved in liquid crystal solvents (LXNMR) has proved to be very useful in this respect [2–5]. Indeed, the averaged dipolar couplings obtained from the spectra contain information on the orientation and conformation of the molecule studied and this has been used in a number of studies [3–14]. The approach used in analysing these experimental data has normally been a model based one, where certain assumptions are made about the intramolecular or the intermolecular interactions. For instance, a single conformer has often been employed in the past [8] and has recently been proposed as a general model [12], on the assumption that the environment around a flexible molecule in a fluid, and in a liquid crystal solvent in particular, is similar to that of a crystal. When applied to LXNMR data, this point of view implies that proton dipolar coupling data for a simple rotameric molecule (for example, biphenyl, bithienyl, etc.) should be and could be fitted, starting from a certain skeletal geometry, by varying the torsional angle.

Other conformational models have appeared in the literature. One consists of assuming a mixture of rigid conformers, typically having *cis*-, *trans*-, but also non-planar orientations ([9] and references therein). Agreement between model and experiment is sought by varying the torsional angles for the various conformers and their weight. Often assumptions have also been made to reduce the number of parameters, for example, about the order parameters of every conformer. For example, the orientational order parameters of the conformers [6, 7, 13] or of a subset of these parameters have been assumed to be the same.

Another important approach, due to Emsley and Luckhurst [15], again considers the flexible molecule as a collection of rigid molecules. However, the number of

*Author for correspondence.

0267–8292/94 $10·00

conformers is now arbitrarily large [10]. The number of parameters, that would be huge, is drastically reduced by assuming that molecular field theory [16] holds for every conformer and estimating the biaxiality of every conformation in some way. In the original method [15], an additivity rule is employed to estimate the parameters of the potential for a conformer in terms of bond contributions. A related treatment that goes beyond the simple bond additivity approximation has been proposed and applied to flexible chains [17]. Mean field treatments based on molecular shape have been introduced by van der Est *et al.* [18], and more recently by Ferrarini *et al.* [19]. It is important to point out that these methods allow for the coupling of orientations and conformations.

A rather different, non-model approach considers a rotameric molecule as made up of fragments that have a certain internal order with respect to a suitable rigid fragment chosen in the molecule [20]. The method [11, 21] then uses the principle of maximum entropy [22] to estimate the flattest orientational-conformational distribution compatible with a certain experimental data set. We have recently extended the method to make it more systematic and to allow for the effect of experimental errors on the distributions obtained, and we have called the procedure maximum entropy internal order (MEIO) [23].

The key point of the MEIO method is to convert a suitable set of experimental observables in an orientational-conformational distribution. Thus the level of detail of the molecular information obtained depends critically on the "quality" of the experimental data examined, as we shall discuss later. To examine this point in detail it is helpful to analyse different sets of data for the same molecule. 2,2′-Bithienyl (DTH) (see figure 1), in itself an important and well-studied molecule [24–36], presents a particularly interesting case from this point of view, since it has been studied with LXNMR by at least three groups at 100 [6–7], 220 [6] and 400 MHz [13]. In particular ter Beek *et al.* [13], have recently performed very careful measurements for 2,2′-bithienyl in a "zero electric field gradient" nematic mixture [13].

Here we wish to apply our model independent MEIO [23] procedure to the DTH system and determine its orientational-conformational distribution. To put our results in perspective we shall give first a brief summary of the findings previously obtained by other authors from the analysis of the dipolar couplings of the DTH molecule.

Khetrapal and Kunwar [6] measured the NMR spectrum of a 14 mol per cent solution of DTH at 100 MHz and 301 K in a nematic mixture of 80 per cent

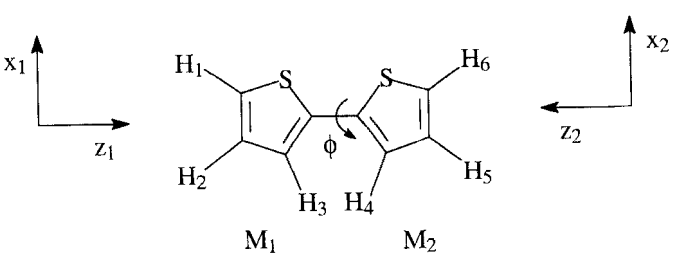

Figure 1. Structure and proton labelling of 2,2′-bithienyl (DTH) together with the coordinate frames of the molecular fragments M_1, M_2. The torsional angle ϕ describes a rotation around z_1 starting from the *cis*-form.

4-ethoxybenzylidene-4'-*n*-butyl aniline and 20 per cent O-carbobutoxy-4-oxybenzoic acid ethoxyphenyl ester. The spectral line width was 6 Hz and the resulting dipolar couplings had an average RMS error of 0·27 Hz. The microwave molecular structure of thiophene [37] was used as a starting skeleton for the two rings. The inter-ring distance was assumed to be $d_{RR}=1{\cdot}49$ Å and the CCC angles containing the inter-ring bond were fixed to 128·7°. Khetrapal and Kunwar [6] could not analyse their data using single rotamer models and invoked a mixture of planar S-*cis*- and S-*trans*-conformers. Using the restriction $(S_{yy})_{cis}=(S_{yy})_{trans}$ on the components S_{ij} of the Saupe ordering matrix [3], they obtained five orientational parameters for the two conformers (two for the *cis*- and three for the *trans*-conformer) and four proton distance ratios (keeping $r_{12}=2{\cdot}64$ Å constant). The relative amounts of the two conformers could not be obtained with a reasonable accuracy. The RMS error between the experimental dipolar couplings and those obtained using these nine parameters was 0·2 Hz.

Bucci *et al.* [7], measured the NMR spectrum of a 20 mol per cent solution of DTH at room temperature in Merck phase IV (*p*-*n*-butyl-*p'*-methoxyazoxybenzene). For the spectrum measured at 100 MHz, 147 lines were determined with an RMS error of 5·3 Hz and a line width of 4 Hz, while for the spectrum at 220 MHz, 149 lines were resolved with an RMS error of 5·1 Hz and a line width of 4 Hz. The resulting dipolar couplings had an average RMS error equal to 1·71 Hz for the 100 MHz spectrum and 1·61 Hz for the 200 MHz one. The molecular structure of DTH determined from X-ray diffraction [24] was used as a fixed skeleton for the two rings and a length $d_{CH}=1{\cdot}08$ Å was assumed for the C–H bonds. Single rotamer models, i.e. planar *cis*- and *trans*-conformers, could not satisfactorily fit the experimental data and a mixture of these planar conformers was assumed. The analysis of the nine available couplings was performed using six variational parameters: five orientational parameters (two for the *cis*- and three for the *trans*-conformer, with the constraints $(S_{zz})_{cis}=(S_{zz})_{trans}$, $(S_{yy})_{cis}=(S_{yy})_{trans}$, $(S_{xz})_{cis}=0$) and one for the conformer population ratio. The analysis of both spectra led to a mixture of 70 per cent *trans* and 30 per cent *cis* with an RMS error between the fitted dipolar couplings and the experimental values of 4·0 Hz for the 100 MHz spectrum and 3·5 Hz for the 220 MHz spectrum.

Ter Beek *et al.* [13], measured the NMR spectrum of DTH at 400 MHz in a nematic solvent formed by 55 per cent w/w Merck ZLI 1132 (eutectic mixture of alkylcyclohexylcyanobenzenes and alkylcyclohexylcyanobiphenyls) and 45 per cent w/w deuteriated EBBA (*d*2(*N*-(*p*-ethoxybenzylidene)-2,6-dideuterio-*p'*-*n*-butyl-aniline)) at 300 K and 304 K. The two 140 line spectra were analysed in terms of nine dipolar couplings giving an RMS error of 0·13 Hz for that at 300 K and 0·16 Hz for that at 304 K. In both cases the line width was 4 Hz. The nine resulting couplings had an average RMS error of 0·034 Hz for the 300 K spectrum and of 0·041 Hz for the 304 K spectrum. These were analysed using a fixed geometry built up from the coordinates of thiophene determined from microwave spectra [37], with $d_{RR}=1{\cdot}455$ Å and the SCC angle between the rings fixed at 119·4° following an MDNO-SCF-MO calculation [32]. Once more, single rotamer models could not fit the experimental data and a mixture of non-planar *cis*- and *trans*-like conformers with dihedral angles ϕ_{cis} and ϕ_{trans} was used. Two sets of analyses were performed. In the first set, ter Beek *et al.* [13], used seven variational parameters: five order parameters (two for the *cis*-like and three for the *trans*-like structures) and two dihedral angles ϕ_{cis} and ϕ_{trans}. In addition they assumed $(S_{xz})_{cis}=0$. The analysis led to $\phi_{cis}=24{\cdot}4°$,

$\phi_{trans}=180{\cdot}0°$ and an RMS error between the fitted and the experimental dipolar couplings of 0·48 Hz for both the 300 K and 304 K data sets, while the weight of the two conformers could not be obtained. For the second kind of analysis, ter Beek *et al.* [13], used five terms: three orientational parameters for the planar *trans*, one dihedral angle ϕ_{cis} and the fractional occupancy p^{trans} for the *trans*-state. In this case ter Beek *et al.* [13], assumed $(S_{yy})_{cis}=(S_{yy})_{trans}$, $(S_{zz})_{cis}=(S_{zz})_{trans}$, $\phi^{trans}=180{\cdot}0°$ and $(S_{xz})_{cis}=0$. The results of the fit were $\phi^{cis}=24{\cdot}1°$, $p^{trans}=0{\cdot}61$ and the RMS error for the fitted couplings was 0·50 Hz for the 300 K data. The analysis of the 304 K data led to $\phi_{cis}=24{\cdot}2°$, $p^{trans}=0{\cdot}61$ and an RMS error of 0·49 Hz. ter Beek *et al.* [13], obtained similar results even on analysing the data from Khetrapal and Kunwar [6] and Bucci *et al.* [7]. They concluded that no solvent effect was present or at least observable.

2. MEIO analysis

The method has been described in detail in [23]. Here we just wish to provide a brief summary, appropriate to the single rotor case treated here, needed to establish the notation and terminology employed later.

2.1. *Dipolar couplings and data analysis*

The proton dipolar couplings D_{ij} determined from the LXNMR experiment can be written in terms of the average of the spherical component of the dipolar coupling tensor along the spectrometer field direction $\langle[T_{ij}]^{2,0}_{\mathrm{LAB}}\rangle$ [3, 20(*b*)]

$$D_{ij}\equiv\left(\frac{2}{3}\right)^{1/2}\langle[T_{ij}]^{2,0}_{\mathrm{LAB}}\rangle, \tag{1a}$$

$$=-\frac{h\gamma_{\mathrm{H}}^2}{4\pi^2}\left\langle\frac{P_2(\cos\theta_{ij})}{r_{ij}^3}\right\rangle, \tag{1b}$$

where γ_{H} is the proton gyromagnetic ratio, r_{ij} is the distance between the two nuclei, θ_{ij} is the angle between the internuclear vector $\mathbf{r}_{ij}$ and the magnetic field direction taken as Z axis. The angular brackets indicate an average over the orientational–conformational distribution. In general r_{ij} and θ_{ij} will depend on the orientation and conformation of the molecule. Assuming uniaxial symmetry of the liquid crystal solvent around the director, the transformation from magnetic (LAB) field to director frame (DIR) can be written as

$$\langle[T_{ij}]^{2,0}_{\mathrm{DIR}}\rangle=P_2(\cos\theta_{\mathrm{DL}})\langle[T_{ij}]^{2,0}_{\mathrm{LAB}}\rangle. \tag{2}$$

The rotation θ_{DL} between magnetic field and director only provides a scaling factor depending on the sign of the diamagnetic anisotropy. Transforming to the M_1 molecular frame placed on the first ('rigid') fragment, we have

$$\langle[T_{ij}]^{2,0}_{\mathrm{DIR}}\rangle=\sum_{n=-2}^{2}\langle D^{2*}_{0n}(\omega)[T_{ij}]^{2,n}_{\mathrm{M_1}}(\phi)\rangle, \tag{3}$$

where $D^2_{mn}(\omega)$ is a Wigner rotation matrix [38] depending on the molecular orientation $\omega\equiv(\alpha,\beta,\gamma)$ in the director frame. If $[T_{ij}]^{2,n}_{\mathrm{M_1}}$ is significantly modulated by the internal rotation then we may hope to obtain some details about the averaging distribution. If we can consider bond distances and angles fixed, the major way of

changing at least some of the dipolar couplings will be by rotating one ring with respect to the other, i.e., by changing the angle ϕ. The information we may get will ultimately depend on the sensitivity of the observable dipolar tensors to ϕ (cf. figure 1).

2.2. *Symmetry*

The spherical components of the dipolar coupling $[T_{ij}]^{2,0}_{\mathrm{DIR}}$ that we have just introduced have implicitly been assumed to be measurable and thus distinguishable from the other nuclear pairs. In practice this will not always be the case, since molecular symmetry coupled to the characteristics of the NMR experiment and its time-scale will reduce the number of observable couplings to those generated by a suitable symmetrization. For instance, in the case of a molecule with two identical fragments, such as DTH, one needs to symmetrize the couplings with respect to their exchange. There are at least two equivalent ways of performing this symmetrization. The first method implements symmetrization with respect to the operations corresponding to the various degrees of freedom, that is the local conformational symmetry of the rotor [39, 40], the symmetry of the whole molecule in an arbitrary conformational state ϕ, the symmetry of the mesophase and that of the NMR experiment. In general we have

$$[T^{\mathrm{S}}_{ij}]^{2,0}_{\mathrm{DIR}}(\omega, \phi)=\frac{1}{n_{\mathrm{s}}}\sum_{S=1}^{n_{\mathrm{s}}}\mathcal{O}_{\mathrm{S}}[T_{ij}]^{2,0}_{\mathrm{DIR}}(\omega, \phi), \tag{4}$$

where $\mathcal{O}_{\mathrm{S}}$ is the projection operator corresponding to each of the n_{S} symmetry operations. The second method, more often used in NMR spectra interpretation, is based on equivalent nuclear pairs and implies averaging over these pairs

$$[T^{\mathrm{S}}_{ij}]^{2,0}_{\mathrm{DIR}}(\omega, \phi)=\frac{1}{n_{\mathrm{p}}}\sum_{P=1}^{n_{\mathrm{p}}}[T_{[ij]_{\mathrm{P}}}]^{2,0}_{\mathrm{DIR}}(\omega, \phi), \tag{5}$$

where $[ij]_{\mathrm{P}}$ is one of the n_{p} equivalent pairs. The two schemes give completely equivalent results. For molecules formed by two indistinguishable rotors one has

$$\langle[T^{\mathrm{S}}_{ij}]^{2,0}_{\mathrm{DIR}}\rangle=\sum_{n=-2}^{2}\left\langle\frac{D^{2*}_{0n}(\omega)+\exp(-in\phi)D^{2*}_{0-n}(\omega)}{2}[T_{ij}]^{2,n}_{\mathrm{M}_1}(\phi)\right\rangle, \tag{6a}$$

$$=\sum_{n=-2}^{2}\left\langle\frac{D^{2*}_{0n}(\omega_1)+D^{2*}_{0n}(\omega_2)}{2}[T_{ij}]^{2,n}_{\mathrm{M}_1}(\phi)\right\rangle, \tag{6b}$$

where ω_1, ω_2 define the orientations of the M_1 and M_2 fragments (defined as in figure 1) with respect to the director frame.

2.3. *Linear independence*

The amount of available information depends on the number of distinguishable nuclear pairs, but clearly not all of them will add new information. Thus, before taking a set of experimental data and analysing them in terms of conformational information, it is important to determine linearly independent combinations. In order to proceed systematically with the choice of observables we have introduced a scalar product between two laboratory fixed dipolar coupling components:

$$([T_I^S]^{2,0}_{DIR}|[T_J^S]^{2,0}_{DIR}) = \int d\omega d\phi [T_I^S]^{2,0}_{DIR}(\omega, \phi) * [T_J^S]^{2,0}_{DIR}(\omega, \phi) \tag{7a}$$

$$= \frac{8\pi^2}{5} \sum_{n=-2}^{2} \int d\phi [T_I^S]^{2,n}_{M_1}(\phi) * [T_J^S]^{2,n}_{M_1}(\phi), \tag{7b}$$

where we use capitalized subscripts $I \equiv \{ij\}$, $J \equiv \{i'j'\}$ as a shorthand way to label a pair of nuclei. Using this definition and a skeleton geometry with N couplings, we can find the dimension n_C of the function space defined by the dipolar couplings using standard techniques of linear algebra. In particular we can define an overlap matrix **V** with elements

$$V_{IJ} = ([T_I^S]^{2,0}_{DIR}|[T_J^S]^{2,0}_{DIR}), \tag{8}$$

The matrix elements are obtained by numerical integration (we use 16 point gaussian), the resulting overlap matrix is diagonalized and the q eigenvalues that are zero within a threshold are discarded. The $n_C = N - q$ eigenvectors corresponding to the non-zero eigenvalues are orthogonal and can be normalized. We call **Z** the $N \times n_C$ matrix containing these n_C eigenvectors as its columns. Thus we identify a set of n_C orthogonalized couplings by the transformation

$$[t_I]^{2,0}_{DIR}(\omega, \phi) = \sum_{J=1}^{N} [T_J^S]^{2,0}_{DIR}(\omega, \phi) Z_{JI}, \tag{9a}$$

$$= \sum_{n=-2}^{2} D^{2*}_{0,n}(\omega) [t_I]^{2,n}_{M_1}(\phi), \tag{9b}$$

where **Z** is the matrix of eigenvectors of **V**. In a similar fashion the transformation equation (9*a*) defines a linear combination d_I of the experimental couplings

$$d_I = \sum_{J=1}^{N} \langle [T_J^S]^{2,0}_{DIR} \rangle Z_{JI}. \tag{10}$$

The quantities $[t_I]^{2,n}_{M_1}(\phi)$ are independent dipolar couplings

$$[t_I]^{2,n}_{M_1}(\phi) = \sum_{J=1}^{N} [T_J^S]^{2,n}_{M_1}(\phi) Z_{JI}, \quad I = 1, \ldots, n_C. \tag{11}$$

We can proceed using these combinations as our observables.

In the case of DTH, the published [6, 7, 13] NMR spectra can be interpreted in terms of the following nine couplings: $T_1^S \equiv \frac{1}{2}(T_{12} + T_{56})$, $T_2^S \equiv \frac{1}{2}(T_{13} + T_{46})$, $T_3^S \equiv \frac{1}{2}(T_{14} + T_{36})$, $T_4^S \equiv \frac{1}{2}(T_{15} + T_{26})$, $T_5^S \equiv T_{16}$, $T_6^S \equiv \frac{1}{2}(T_{23} + T_{45})$, $T_7^S \equiv \frac{1}{2}(T_{24} + T_{35})$, $T_8^S \equiv T_{25}$, $T_9^S \equiv T_{34}$.

In practice we have used an eigenvalue threshold of $10^{-4}\,\mathrm{kHz}^2$. This amounts to neglecting linear combinations whose average value when integrated over $\{\beta, \gamma, \phi\}$ is below 10 Hz. For all the molecular geometries employed (see later), seven linearly independent combinations t_I could be extracted from the nine T_I^S. We show in table 1 the percentage compositions of the t_I in terms of the couplings T_I^S obtained using the geometry of [13].

3. Maximum entropy distributions

The LXNMR experiment determines averages of a set of dipolar couplings or rather of their orthogonalized combinations d_I over the orientational conformational

Table 1. Percentage contribution of the different symmetrized couplings T_I^S to the orthogonal combinations t_I obtained using DTH coordinates from ter Beek *et al.* [13].

	t_1	t_2	t_3	t_4	t_5	t_6	t_7
T_1^S	36·35	52·42	8·97	1·45	0·00	0·67	0·06
T_2^S	0·02	4·95	0·09	42·36	0·00	42·06	3·98
T_3^S	0·31	0·03	0·00	22·58	54·53	15·90	6·19
T_4^S	0·07	0·01	0·00	1·30	1·11	0·60	20·74
T_5^S	0·07	0·04	0·00	0·00	0·69	6·34	64·25
T_6^S	58·01	38·82	0·18	0·32	0·04	1·69	0·42
T_7^S	0·37	0·05	1·35	26·71	41·64	28·55	0·51
T_8^S	0·08	0·00	0·06	3·71	1·35	4·15	3·85
T_9^S	4·71	3·69	89·35	1·57	0·64	0·04	0·00

distribution $P(\omega, \phi)$. Thus, according to maximum entropy [22], the best (least biased) approximation to the true distribution in the uniaxial mesophase obtainable from an LXNMR will be of the form

$$P(\omega, \phi) = \exp\left\{\sum_{I=1}^{nC} \lambda_I [t_I]^{2,0}_{DIR}(\omega, \phi)\right\} \Big/ Z_0, \tag{12}$$

where Z_0 is defined by

$$Z_0(\{\lambda_I\}) = \int d\omega d\phi \exp\left\{\sum_{I=1}^{nC} \lambda_I [t_I]^{2,0}_{DIR}(\omega, \phi)\right\}. \tag{13}$$

The quantity in the exponent in equation (13) plays the role of an effective orientation-conformational potential and the coefficients λ_I will be determined from the condition that they should give the experimental observables d_K, linear combinations of the $\langle [T_J^S]^{2,0}_{DIR}\rangle$ (equation (10)), by integration, i.e. that

$$d_K = \frac{\int d\omega d\phi [t_K]^{2,0}_{DIR}(\omega, \phi) \exp\{\sum_I \lambda_I [t_I]^{2,0}_{DIR}(\omega, \phi)\}}{\int d\omega d\phi \exp\{\sum_I \lambda_I [t_I]^{2,0}_{DIR}(\omega, \phi)\}}. \tag{14}$$

It is apparent that when only one average dipolar coupling is determined, the functional form of the distribution is a direct consequence of the angular form of that dipolar coupling. As the number of independent observables increases, the effective potential can take any form that can be expressed as a linear combination of the basis set in equation (9). Even though the basis is not complete, it can certainly accommodate a variety of effective potentials. The practical determination of the best distribution, i.e. of the best set of λ_I, is performed defining a suitable functional [22(b)]

$$\Gamma(\{\lambda_I\}) = \ln Z_0(\{\lambda_I\}) - \sum_{I=1}^{nC} \lambda_I d_I \tag{15}$$

using the experimental observables (dipolar coupling independent combinations) and Z_0. The problem of solving the system of non-linear equations (14) is converted to that of finding the set of $\{\lambda_I\}$ that minimizes Γ. It is worth noticing that the use of orthogonalized couplings, apart from reducing the correlation between parameters, is also numerically convenient, since it decreases the number of parameters to be

minimized. From a practical point of view we perform the minimization using a quasi-Newton method as described in [23]. In any case, the output coefficients $\{\lambda_l\}$ define the orientational-conformational distribution $P(\beta, \gamma, \phi)$ compatible with the experimental data, which is then integrated over β, γ to give $P(\phi)$ [23].

3.1. *Error analysis*

The effect of experimental errors on the conformational data has been determined using a sampling method [23]. We start from the N available dipolar couplings and their experimental standard deviation and we generate M data sets (for DTH we used $M = 50$) by sampling from N gaussians of width σ_i centred at the observed values, as described in detail in [23]. Each data set generated is then analysed with the algorithm described earlier to obtain a distribution $P_i(\beta, \gamma, \phi)$. Each of the M distributions obtained is used to calculate a $P_i(\phi)$ which can then be employed to obtain an average distribution $\bar{P}(\phi)$ and the attendant standard deviation at each ϕ. This error bar for each ϕ gives rise to the shaded error area for the distributions shown in figure 2. The errors on the order parameters are obtained similarly by calculating order parameter values from each distribution and calculating their average and standard deviation. We have also routinely performed the analysis of the central data set and have found that $P(\phi)$ and $\bar{P}(\phi)$, although not identical, are quite similar for the case we have treated.

4. Results

The experimental dipolar couplings measured by Khetrapal and Kunwar [6], Bucci *et al.* [7], and ter Beek *et al.* [13], have been analysed with the MEIO method as described in the previous section and using the geometry of [13]. The order parameters $\mathrm{Re}\langle D^2_{0n}\rangle$ determined in this way are reported in table 2. The agreement between experimental couplings and those recalculated with the MEIO distribution is excellent, as we can see from the errors reported in table 3. The conformational distributions $\bar{P}(\phi)$ for the three cases are shown in figure 2 together with their error bands. We notice that the distribution obtained starting from the data of Khetrapal and Kunwar [6], figure 2 curve (*a*), appears to be nearly isotropic and shows a rather large uncertainty. This is due, at least in part, to the low degree of order of the nematic solvent employed in the experimental conditions. The DTH order parameter was $\langle P_2\rangle = 0{\cdot}15$.

Turning now to the $\bar{P}(\phi)$ data for Bucci *et al.* [7], we see that these also have a very large uncertainty band. The distributions at (*b*) 100 and (*c*) 220 MHz still appear rather flat. The solute order is rather low also in this case ($\langle P_2\rangle = 0{\cdot}24$), and consequently the reliability of the information obtained is limited.

In the case of the ter Beek *et al.* [13], 300 K data (*d*), the experimental errors are very small and the error bands obtained are practically invisible on our scale. This can be due in part to the higher order parameter ($\langle P_2\rangle = 0{\cdot}37$). It is important to notice that the MEIO distribution $\bar{P}(\phi)$ has a peak at $\phi = 180°$ and a lower one at $\phi \approx 20°$, in excellent agreement with what has been determined in [13]. The other data set from ter Beek *et al.*, at 304 K, gave very similar results to those of figure 2(*d*) and thus is not reported here.

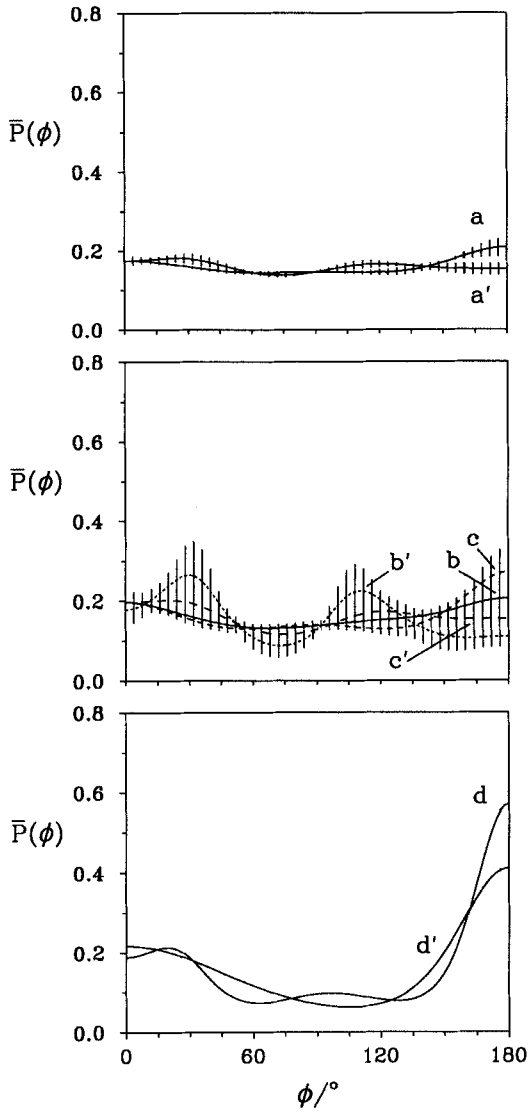

Figure 2. Torsional angle distributions $\bar{P}(\phi)$ with their errors bars obtained from an MEIO analysis of data from Khetrapal and Kunwar [6] (*a*), (*a'*); Bucci *et al.* [7], at 100 MHz (*b*), (*b'*) and at 220 MHz (*c*), (*c'*); ter Beek *et al.* [13], (*d*), (*d'*). Curves with a primed (unprimed) label are derived using coordinates from [7] ([13]).

4.1. *Reliability tests*

4.1.1. *Recovery of mono-rotamers*

We have checked the ability of the MEIO method actually to obtain a single-conformer or *cis-trans*-mixture if one exists as described in [23]. Thus we have generated simulated average dipolar couplings similar to the actual experimental data of [13], by integrating the $[T_{ij}]^{2;0}_{DIR}(\beta, \gamma, \phi)$ with a distribution corresponding to orientational order parameter $\langle P_2 \rangle = 0{\cdot}36$, $\mathrm{Re}\langle D^2_{01} \rangle = -0{\cdot}0006$ and $\mathrm{Re}\langle D^2_{02} \rangle$

Table 2. Orientational order parameters $\mathrm{Re}\langle D^2_{0,m}\rangle$ for DTH obtained by analysing the NMR couplings from Khetrapal and Kunwar [6] (*a*); Bucci *et al.* [7], 100 MHz (*b*) and 220 MHz (*c*); ter Beek *et al.* [13], (*d*). DTH coordinates from ter Beek *et al.* [13].

	(*a*)	(*b*)	(*c*)	(*d*)
$\langle D^2_{0,0}\rangle$	0·1509±0·0003	0·223±0·001	0·220±0·001	0·3658±0·0001
$\mathrm{Re}\langle D^2_{0,1}\rangle$	0·0279±0·0002	0·039±0·001	0·037±0·001	0·0743±0·0001
$\mathrm{Re}\langle D^2_{0,2}\rangle$	0·0077±0·0004	0·013±0·002	0·012±0·002	−0·0006±0·0001

=0·07 for DTH. As we have already mentioned, taking into account the effect of orientational disorder is quite important, since the sensitivity of the method decreases as $\langle P_2\rangle$ decreases and after all no information can be obtained when $\langle P_2\rangle=0$. We have found the results collected in figure 3 for mono-rotamers at various torsional angles (top plate) and for the *cis–trans*-combination found in [13] (bottom plate). We observe first of all that the MEIO distributions are always broader than the input distributions [11] as we might expect, since the maximum entropy distribution is at any stage the flattest compatible with a set of experimental data. It is also clear that a true mono-rotameric distribution, with a Dirac's delta form $\delta(\phi-\phi_0)$ cannot be reconstructed from a limited number of harmonics. Indeed the Fourier expansion of a delta function contains an infinite number of these harmonics and cannot strictly be written in our limited basis set of $[t_1]^{2;m}_{M_1}(\phi)$. However, it is sufficient for our purposes to compare the form of $P(\phi)$ obtained with the assumed single conformer or *cis–trans* input with that obtained from the analysis of experimental data (cf. figure 2(*d*)). We see in particular that none of the mono-rotamer distributions (*a*)-(*f*) resembles the one obtained from the experimental data. On the other hand, all the curves present a more or less broad peak in correspondence with the assigned conformer angle, so that a single conformer could be found if it was really present. We also see, using as input to the simulated data a

Table 3. Results for the MEIO analysis of the experimental NMR dipolar couplings D_I for the DTH molecule measured by Khetrapal and Kunwar [6] (*a*); Bucci *et al.* [7], 100 MHz (*b*) and 220 MHz (*c*); ter Beek *et al.* [13], (*d*). The MEIO analyses have been performed using the coordinates from [13].

D_I	Expt. (*a*) /Hz	Calc./Hz	Expt. (*b*) /Hz	Calc./Hz	Expt. (*c*) /Hz	Calc./Hz	Expt. (*d*) /Hz	Calc./Hz
1	291·60	291·62	454·10	454·10	454·40	454·40	614·68	614·68
2	−43·60	−43·76	−58·60	−58·61	−59·70	−59·72	−148·09	−148·08
3	−88·90	−88·94	−131·30	−131·33	−130·80	−130·83	−216·24	−216·32
4	−34·50	−34·29	−51·20	−50·86	−50·20	−49·92	−84·15	−83·20
5	−28·90	−28·55	−41·50	−41·25	−41·80	−41·57	−79·92	−72·26
6	−866·20	−866·18	−1267·20	−1267·21	−1257·10	−1257·11	−2189·46	−2189·50
7	−81·60	−81·52	−118·10	−118·08	−115·50	−115·48	−184·19	−184·14
8	−34·90	−35·65	−52·20	−52·41	−51·30	−51·53	−82·31	−82·74
9	−332·90	−332·90	−470·70	−470·70	−462·50	−426·50	−741·47	−741·47
	RMS error = 0·31 Hz		RMS error = 0·17 Hz		RMS error = 0·15 Hz		RMS error = 0·44 Hz	

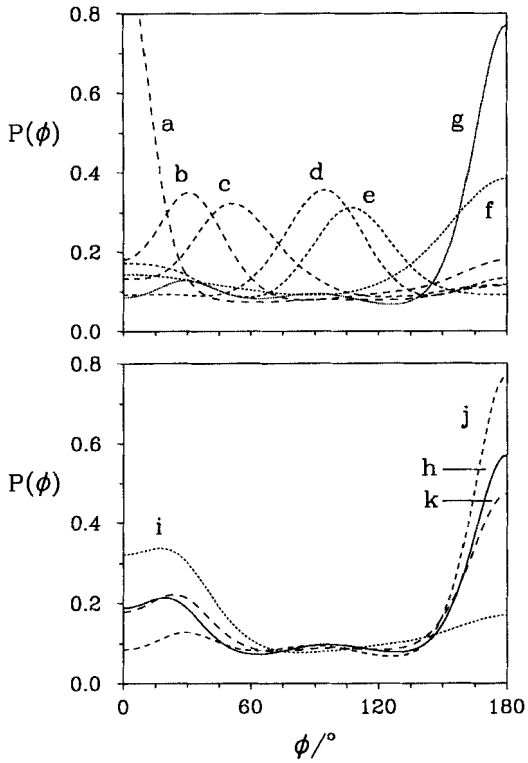

Figure 3. Results of MEIO analysis of simulated single conformer distributions at $\phi = 0°$ (*a*), 30° (*b*), 60° (*c*), 90° (*d*), 120° (*e*), 150° (*f*), 180° (*g*) (top plate). In the bottom plate results of MEIO analysis of simulated single conformer distributions at $\phi = 24{\cdot}2°$ (*i*), 180° (*j*) and simulated *cis*-trans-mixture with $\phi_{cis} = 24{\cdot}2°$ and $p^{trans} = 0{\cdot}61$ (*k*). The curve (*h*) represents the MEIO analysis of data of ter Beek *et al.* [13]. All the results are derived using coordinates from [13].

cis-trans-like mixture with $\phi_{cis} = 24{\cdot}2°$ and $p^{trans} = 0{\cdot}61$ (see figure 3 bottom), that the MEIO method actually gives back a *cis-trans*-distribution with a *trans*-dominance, even though a somewhat broadened one with respect to the input distribution. We conclude that the MEIO distribution supports that obtained by ter Beek *et al.* [13].

4.1.2. *Effect of geometry*

The results obtained from a MEIO analysis of the NMR dipolar couplings are clearly dependent on the molecular geometry employed. We have studied the influence of this factor by re-analysing the various sets of data [6, 7, 13] using the geometry proposed by Bucci *et al.* [7]. In all cases we have found, as we see in table 4, that the RMS error of the fitted to experimental couplings is higher than in the case of the previous analyses performed with the geometry of [13], shown in table 3. In figure 2 we also show the conformational distributions $\bar{P}(\phi)$ obtained with the geometry of [7]. We see that the rather flat distributions obtained from the data of Khetrapal and Kunwar [6] (curves *a*, *a'*) do not show appreciable differences. In the case of the data of Bucci *et al.* [7], the $\bar{P}(\phi)$ appear to be slightly different. In particular the peaks at $\phi \approx 25°$ and $\phi \approx 115°$ of the $\bar{P}(\phi)$ for the 100 MHz data

Table 4. Same as table 3 but with the MEIO analyses performed using the coordinate set from [7].

D_i	Expt. (*a*) /Hz	Calc./Hz	Expt. (*b*) /Hz	Calc./Hz	Expt. (*c*) /Hz	Calc./Hz	Expt. (*d*) /Hz	Calc./Hz
1	291·60	291·70	454·10	454·23	454·40	454·52	614·68	614·84
2	−43·60	−44·63	−58·60	−59·94	−59·70	−61·02	−148·09	−149·75
3	−88·90	−88·80	−131·30	−131·13	−130·80	−130·63	−216·24	−216·02
4	−34·50	−37·00	−51·20	−54·99	−50·20	−53·94	−84·15	−88·88
5	−28·90	−29·59	−41·50	−42·81	−41·80	−43·10	−72·92	−74·56
6	−866·20	−865·91	−1267·20	−1266·81	−1257·10	−1256·71	−2189·46	−2188·97
7	−81·60	−81·41	−118·10	−117·90	−115·50	−115·30	−184·19	−183·94
8	−34·90	−37·15	−52·20	−54·76	−51·30	−53·81	−82·31	−85·47
9	−332·90	−332·90	−470·70	−470·70	−462·50	−462·50	−741·47	−741·47
	RMS error = 1·27 Hz		RMS error = 1·76 Hz		RMS error = 1·73 Hz		RMS error = 2·18 Hz	

(curve *b'*) now appear more pronounced. However, we should notice that the distributions corresponding to the different geometries fall essentially within the same error band, so that the results cannot be considered as significantly different.

Finally, we consider the effect of the same change of geometry on the distribution obtained from the data of ter Beek *et al.* [13]. We see that both functions (*d*, *d'*) have a pronounced maximum for $\phi = 180°$, while the peak at $\phi \approx 20°$ obtained with the coordinate of [13] is replaced by a broad hump centred at $\phi = 0°$.

4.1.3. *Eigenvalue threshold*

We have repeated the analyses of the dipolar couplings of [6, 7, 13] using acceptance thresholds of $10^{-3}\,kHz^2$ and $10^{-2}\,kHz^2$, which cause a reduction in the number of linearly independent combinations t_i to 6 and 5, respectively. In practice this means a progressive reduction of the contribution from the couplings that are less strongly dependent on ϕ. All the resulting distributions become flatter, which can be understood, since less input information is employed and less variational parameters are used. Thus it might be tempting to use a very small threshold to use the available experimental data fully. In practice it turns out that lowering the threshold below $10^{-4}\,kHz^2$ does not improve the results of the analysis.

4.2. *Roto-conformational analysis*

The MEIO procedure does not just yield the conformational distribution $\bar{P}(\phi)$, but an approximation to the full orientational-conformational distribution $\bar{P}(\beta, \gamma, \phi)$. A clear representation of $\bar{P}(\beta, \gamma, \phi)$ and of its attendant uncertainty is not easy. We have chosen to represent $\bar{P}(\beta, \gamma, \phi)$ as a three-dimensional plot of $\bar{P}(\beta, \gamma)$ (see figure 4) with a regular grid for the angles β and γ where each orientation is further colour coded, as shown in the palette in figure 4, to indicate the torsional angle corresponding to the maximum of the normalized distribution

$$\bar{P}'(\beta, \gamma, \phi) = \frac{\bar{P}(\beta, \gamma, \phi)}{\int d\phi \bar{P}(\beta, \gamma, \phi)}. \tag{16}$$

However, it is important to appreciate that this can be rather misleading when the peak is very broad. Thus we have further colour coded the standard deviation σ as

shown in the figure 4, so that a full bright colour represents an angular distribution with $\sigma < 30°$ and an increasingly dark colour corresponds to larger uncertainties according to the palette shown. The colour scheme is designed so that all the width codes go to the same dark tone when the uncertainty (broadness of the peak) is so large ($\sigma > 50°$) as to make the definition of the peak and its associated colour essentially useless.

In this representation, a mono-rotamer would correspond to a $\bar{P}(\beta, \gamma)$ with a uniform colour corresponding to its torsional angle. A grey area would correspond to a lack of reliable information on the internal angle. A $\bar{P}(\beta, \gamma)$ with different well defined colours as in figure 4(*a*) corresponds to different internal angles being favoured at different orientations, and thus to orientation–conformation coupling. In figure 4(*a*) we show the orientational–conformational distribution obtained applying the MEIO procedure to the data of Bucci *et al.* [7], at 100 MHz using their original coordinate set. This would correspond to the $\bar{P}(\phi)$ shown in figure 2(*b*′). As we can observe, the plot presents various coloured regions corresponding to a different preferred torsional angle as the overall orientation of the molecule with respect to the director β, γ, changes. We believe that this novel kind of representation of the data could be useful in a variety of circumstances. In this specific case, however, we have seen that the data of [7] corresponded to rather low order, which might have been connected with having the orientational and conformational barrier of comparable height.

In the case of the data of ter Beek *et al.* [13], the $\bar{P}(\beta, \gamma)$ distribution obtained with the MEIO method is presented in figure 4(*b*). In this case the dominant blue colour shows the dominance of the *trans*-conformation and in general little orientational–conformational coupling appears to exist.

5. Discussion

2,2′-Bithienyl has been studied with X-rays in the solid state and found to be planar with an S-*trans*-form [24]. Electron diffraction studies [30] find instead nearly free rotation or motion over low barriers (smaller than $\approx 0{\cdot}5$ kcal) in the gas phase. Molecular orbital calculations [25] also suggest free rotation, with energy minima smaller than 1 kcal mol^{-1}. Another subsequent theoretical study [27] again predicted fairly low barriers, but a preference for the S-*cis*-conformation. The most recent theoretical calculations we are aware of, obtained at STO31G* [35] level, predict yet another different result: an energy minimum at 150° and a less pronounced one at 40°. It is tempting to try and compare right away these findings with the results from the MEIO analysis. We notice, however, that the interpretation of $P(\phi)$ should be considered rather carefully and in particular that $P(\phi)$ cannot be simply interpreted in terms of a potential barrier related only to the changes in energy upon rotating the second ring with respect to the first one. Indeed this would be equivalent to saying that orientational and conformational order are decoupled. In a fluid, $P(\phi)$ is a result of integrating the conformational distribution at every angle $P(\beta, \gamma, \phi)$ over the molecular orientations. To examine this point we have plotted in figure 5 the angle resolved distribution $\bar{P}(\beta, \gamma, \phi)$, corresponding to the case of figure 2(*d*), at a few selected orientations β and for a fixed angle $\gamma_0 = 15°$. As we see the probability of having a certain conformational angle ϕ is somewhat sensitive to the molecular orientation. This in turn is reasonable when the barriers to overall rotation and to conformational change are similar.

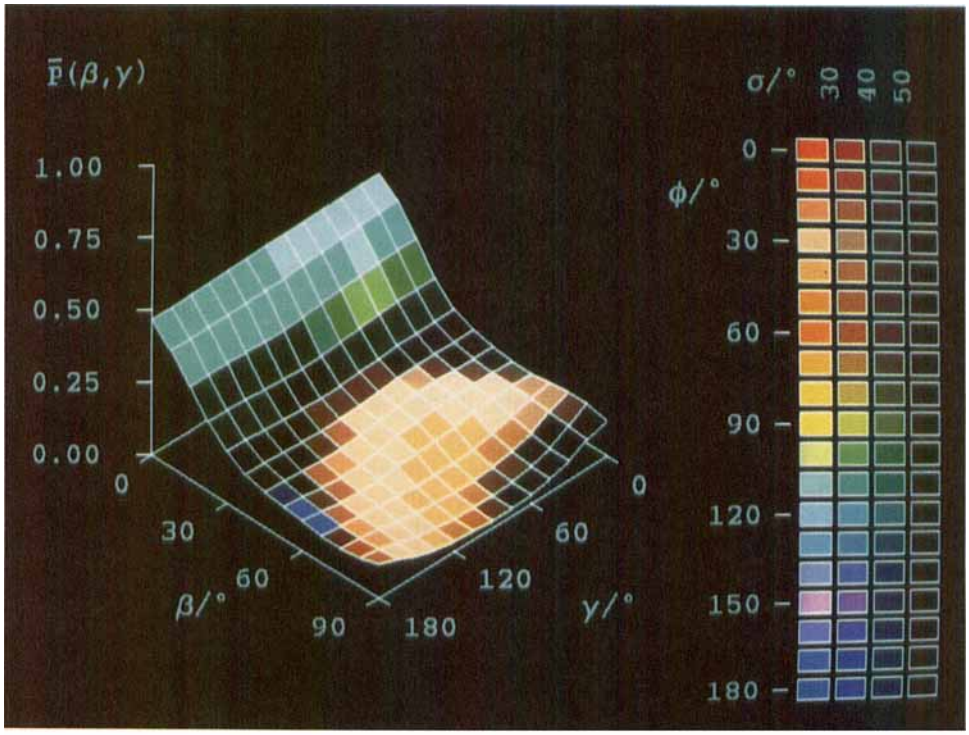

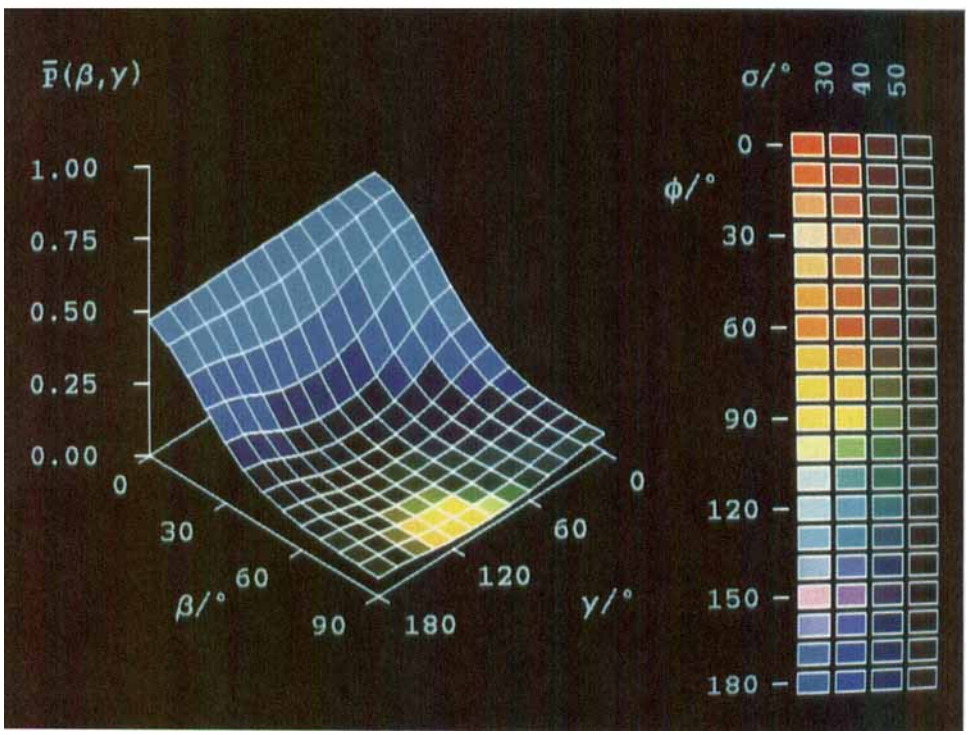

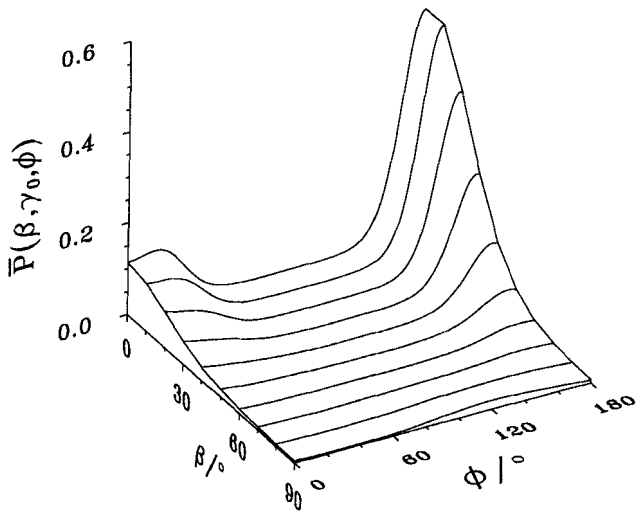

Figure 5. Plot of the orientational-conformational distribution $\bar{P}(\beta, \gamma_0, \phi)$ with $\gamma_0 = 15°$ for some selected orientations β as obtained from data and coordinates of ter Beek *et al.* [13].

The overall appearance of $\bar{P}(\phi)$ as shown in figure 2(*d*) could result from the effect of having more than one potential minimum when rotating around the interring axis, as well as being a consequence of superimposing the minima at different orientations. Notice also that the presence of roto-conformational coupling has the consequence that the purely orientational order parameters are influenced by the internal motion. The values that the ordering matrix determined for a fragment assume are dependent on the total molecular symmetry and not just on that of the fragment.

The MEIO approach does not make assumptions that all or part of the order parameters of different conformers are equal. It is comforting to see that in this case the information obtained in this rather straightforward and model independent way is in excellent agreement with the results obtained from the more *ad hoc* treatment of [13].

6. Conclusions

The acquisition of conformational information in solution without preliminary model assumptions is possible and has been demonstrated for a practically important case, that of DTH. It seems to us that now that the data analysis methodology is ready and available, what is mostly needed is a fresh, accurate series of experimental

Figure 4. Three-dimensional plots of $\bar{P}(\beta, \gamma)$ as obtained from the analysis of data of Bucci *et al.* [6] (top plate), and ter Beek *et al.* [13] (bottom plate), using in both cases the sets of coordinates reported in the original papers. For each couple β, γ corresponding to a cell of the surface, a colour taken from the palette shown is assigned, computing the torsional angle and the variance σ associated with the highest peak of the normalized distribution given in equation (16).

determinations for molecules of interest. From this point of view we find extremely promising the recent development of techniques like those of Pines *et al.* [14] that allow sets of dipolar couplings for more complex molecules to be obtained. We have also developed a few tools for representing and studying the orientational-conformational coupling, and it would be timely to see this important effect more systematically investigated. We stress that care should be taken when performing experiments aimed at obtaining conformational information in avoiding too low ordering of the solute of interest.

We wish to thank CNR and MURST (Rome) for support of this work.

References

[1] For a recent overview see, 1992, *Faraday Symposium 27*, The conformation of flexible molecules in fluid phases, *J. chem. Soc. Faraday Trans.*, **88**.
[2] DIEHL, P., and KHETRAPAL, C. L., 1969, *NMR Basic Principles and Progress*, Vol. 1, edited by P. Diehl, E. Fluck and R. Kosfeld (Springer-Verlag).
[3] EMSLEY, J. W., and LINDON, J. C., 1975, *NMR Spectroscopy Using Liquid Crystal Solvents* (Pergamon Press).
[4] LUNAZZI, L., 1976, *Determination of Organic Structures by Physical Methods*, Vol. 6, edited by F. C. Nachod, J. J. Zuckermann and E. W. Randall (Academic Press, London), p. 335.
[5] EMSLEY, J. W. (editor), 1985, *Nuclear Magnetic Resonance of Liquid Crystals* (Reidel).
[6] KHETRAPAL, C. L., and KUNWAR, A. C., 1974, *Molec. Phys.*, **28**, 441.
[7] BUCCI, P., LONGERI, M., VERACINI, C. A., and LUNAZZI, L., 1974, *J. Am. chem. Soc.*, **96**, 1305.
[8] FIELD, L. D., and STERNHELL, S., 1981, *J. Am. chem. Soc.*, **103**, 703.
[9] VERACINI, C. A., and LONGERI, M., 1985, *Nuclear Magnetic Resonance of Liquid Crystals*, edited by J. W. Emsley (Reidel), Chap. 7, p. 123.
[10] CELEBRE, G., LONGERI, M., and EMSLEY, J. W., 1988, *J. chem. Soc. Faraday Trans. II*, **84**, 1041.
[11] CATALANO, D., DI BARI, L., VERACINI, C. A., SHILSTONE, G. N., and ZANNONI, C., 1991, *J. chem. Phys.*, **94**, 3928.
[12] (a) GALLAND, D., and VOLINO, F., 1991, *J. Phys.*, **1**, 209. (b) VOLINO, F., and GALLAND, D., 1992, *Molec. Crystals liq. Crystals*, **212**, 77.
[13] TER BEEK, L. C., ZIMMERMAN, D. S., and BURNELL, E. E., 1991, *Molec. Phys.*, **74**, 1027.
[14] ROSEN, M. E., RUCKER, S. P., SCHMIDT, C., and PINES, A., 1993, *J. phys. Chem.*, **97**, 3858.
[15] (a) EMSLEY, J. W., and LUCKHURST, G. R., 1980, *Molec. Phys.*, **41**, 19. (b) EMSLEY, J. W., LUCKHURST, G. R., and STOCKLEY, C. P., 1982, *Proc. R. Soc.* A, **381**, 117.
[16] LUCKHURST, G. R., ZANNONI, C., NORDIO, P. L., and SEGRE, U., 1975, *Molec. Phys.*, **30**, 1345.
[17] PHOTINOS, D. J., SAMULSKI, E. T., and TORIUMI, H., 1992, *J. chem. Soc. Faraday Trans.*, **88**, 1875.
[18] VAN DER EST, A. J., KOK, M. Y., and BURNELL, E. E., 1987, *Molec. Phys.*, **60**, 397.
[19] FERRARINI, A., MORO, G. J., NORDIO, P. L., and LUCKHURST, G. R., 1992, *Molec. Phys.*, **77**, 1.
[20] ZANNONI, C., 1985, *Nuclear Magnetic Resonance of Liquid Crystals*, edited by J. W. Emsley (Reidel, Dordrecht), (a) Chap. 2, (b) Chap. 1.
[21] DIBARI, L., FORTE, C., VERACINI, C. A., and ZANNONI, C., 1987, *Chem. Phys. Lett.*, **143**, 263.
[22] (a) LEVINE, R. D., and TRIBUS, M. (editors), 1979, *The Maximum Entropy Formalism* (MIT Press). (b) MEAD, L. R., and PAPANICOLAU, B., 1984, *J. math. Phys.*, **25**, 2404.
[23] BERARDI, R., SPINOZZI, F., and ZANNONI, C., 1992, *J. chem. Soc. Faraday Trans.*, **88**, 1863.
[24] VISSER, G. J., HEERES, G. J., WOLTERS, J., and VOS, A., 1968, *Acta crystallogr.* B, **24**, 467.
[25] SKANCKE, A., 1970, *Acta chem. scand.*, **24**, 1389.
[26] ARONEY, M. J., LEE, H. K., and LE FEVRE, R. J. W., 1972, *Aust. J. Chem.*, **25**, 1561.

[27] GALASSO, V., and TRINAJSTIC, N., 1972, *Tetrahedron*, **28,** 4419.
[28] NORDEN, B., HAKANSSON, R., and SUNDBOM, M., 1972, *Acta chem. scand.*, **26,** 429.
[29] MEUNIER, P., COUSTALE, M., GUIMON, C., and PFISTER-GUILLOZO, G., 1977, *J. molec. Struct.*, **36,** 243.
[30] BASTIANSEN, O., KVESETH, K., and MØLLENDAL, H., 1979, *Topics in Current Chemistry*, Vol. 81 (Springer-Verlag), p. 99.
[31] ABU-EITTAH, R. H., and AL-SUGEIR, F. A., 1985, *Bull. chem. Soc. Japan*, **58,** 2126.
[32] BRÉDAS, J. L., STREET, G. B., THEMANS, B., and ANDRE, J. M., 1985, *J. chem. Phys.*, **83,** 1323.
[33] BARONE, V., LELJ, F., RUSSO, N., and TOSCANO, M., 1986, *J. chem. Soc. Perkin Trans. II*, 907.
[34] JONES, D., GUERRA, M., FAVARETTO, L., MODELLI, A., FABRIZIO, M., and DISTEFANO, G., 1990, *J. phys. Chem.*, **94,** 5761.
[35] DISTEFANO, G., DALCOLLE, M., JONES, D., ZAMBIANCHI, M., FAVARETTO, L., and MODELLI, A., 1993, *J. phys. Chem.*, **97,** 3504.
[36] BELJONNE, D., SHUAI, Z., and BRÉDAS, J. L., 1993, *J. chem. Phys.*, **98,** 8819.
[37] BAK, B., CHRISTENSEN, D., HANSEN-NYGAARD, L., and RASTRUP-ANDERSEN, J., 1961, *Molec. Phys.*, **28,** 441.
[38] ROSE, M. E., 1957, *Elementary Theory of Angular Momentum* (Wiley).
[39] MARUANI, J., HERNANDEZ LAGUNA, A., and SMEYERS, Y. G., 1975, *J. chem. Phys.*, **63,** 4515.
[40] ALTMANN, S. L., 1977, *Induced Representations in Crystals and Molecules* (Academic Press).